International Journal of Scientific Engineering and Research (IJSER)
www.ijser.in
ISSN (Online): 2347-3878, Impact Factor (2014): 3.05

# Supervised Learning Approach for Performance Evaluation of Digital Fundus Image Quality

**P. Syed Ali Fathima Aasia[1], K. Gokulakrishnan[2], J. Jesu Vedha Nayahi[3]**

[1]PG Scholar, Department of Electronics & Communication Engineering, Regional Center, Anna University, Tirunelveli Region, Tirunelveli, Tamilnadu, India

[2]Assistant Professor, Department of Electronics & Communication Engineering, Regional Center, Anna University, Tirunelveli Region, Tirunelveli, Tamilnadu, India

[3]Assistant Professor, Department of Computer Science and Engineering, Regional Center, Anna University, Tirunelveli Region, Tirunelveli, Tamilnadu, India

**Abstract:** ***The fundus image quality is an important parameter in medical applications. Low quality of fundus images can affect to perform a correct diagnosis. In earliest method, to estimate the fundus image quality in local image analysis technique. Drawback of this method it is only applicable for small dataset and affected some factors in retina features. To prevent those limitations we proposed a new method to determine the quality of retinal image whether it is good or bad. Initially preprocessing stage has been employed and calculates the mask .To estimate the focus measures are extracted from each image, then all focus measure values are plotted into box plot because we can predict the rules and assigned to the classifier and classify it. Finally, to obtain the classifier performance is achieved by receiver operating characteristic (ROC) curve.***

**Keywords:** Mask, Focus Measure, Box Plot, Classification

## 1. Introduction

The fundus of the eye is the interior surface of the eye, opposite the lens, and includes the retina, optic disc, macula and fovea, and posterior pole. The term fundus may also be inclusive of bruch's membrane and the choroid. In one study of primates the retina is blue, green, yellow, orange, and red. only the human fundus is red. The major differences were size and regularity of the border of macular area, size and shape of the optic disc, apparent 'texturing' of retina, and pigmentation of retina [1-3]. The eye's fundus is the only part of the human body where the microcirculation can be observed directly. The diameter of the blood vessels around the optic disc is about 150µm, and an ophthalmoscope allows observation of blood vessels with diameters as 10 µm. Measuring the quality of the image is a complicated and hard process since humans opinion is affected by physical and psychological parameters [4-5]. It includes five aspects of retinal image quality .They are focus and clarity, field definition, visibility of the optic disc, visibility of the macula and artifacts. In existing methods like histogram based methods [6], image structure clustering [7] and local image analysis [8] is to verify the retina image quality in order to segmentation, used to filter bank and to extract region growing correspondence with patches. In all those methods we have several shortcomings. It is applicable for small set of dataset, affecting retina factors like field of view, optic diameter, haze, dust and dirt, lashes, arcs, uneven illumination over macula, uneven illumination over edge, uneven illumination over optic disc, and total blink [9-12]. To overcome these limations we introduced a new proposed method like supervised learning based on focus features is to verify the fundus image quality. The proposed method starts with calculate the mask and extracted the features like focus measure and it classifies fundus image quality through the various classifier and it is calculated the system performance.

## 2. Mask

Masking can describe either the techniques or materials used to control the development of a work of art by protecting a desired area from change or a phenomenon that causes a sensation to be concealed from conscious attention. There are two types of mask algorithm one is Clinically Relevant Mask (CRM) and other is Noise Mask (NM).

### 2.1 Clinically Relevant Mask (CRM)

The green plane image is used to calculate the FOV (field of view) mask since it corresponds to the plane with more contrast. Following, a binary mask is generated to extract the FOV. As the FOV area remains equal for all images acquired from the same equipment, a unique mask is created for each database and then used to all images [13]. We have chosen the threshold with high intensity value of that image. Figure 1 shows that the works flow of the clinically relevant mask.

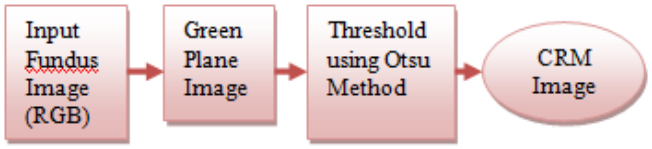


**Figure 1:** Work Flow of the CRM

### 2.2 Noise Mask (NM)

It involves two steps. The following steps are briefly described below:

i) Green Plane Image used to obtain the binary mask of bright regions, a dynamic threshold, t1 needs to be determined. The parameter threshold t1 is the intensity value corresponding to the percentage P1 of the brighter pixels extracted. This figure 2 shows that the work flow of the noise mask with green plane.

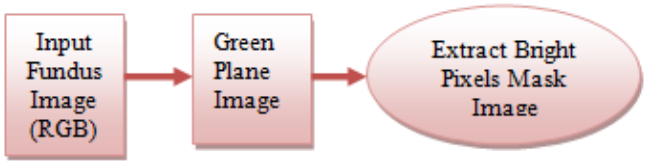


**Figure 2:** Work Flow of the NM with Green Plane

ii) To segment the dark regions, we followed a similar approach, but first it was necessary to transform the dark regions into bright. The conversion of the original RGB (Red Green Blue) fundus image to the CMYK (Cyan Magenta Yellow Black) color space allowed us to obtain the wanted effect in the black component, as the bright objects appear as dark and the dark as bright. The black plane of CMYK color space was used in the following calculations. To obtain the binary mask of the dark regions two dynamic thresholds, t2 and t3, are determined. First, the parameter t2 corresponds to the image brightness and is obtained. Then, if t2 is higher than a fixed value, x1, t3 is determined as the intensity value corresponding to the percentage P2 of the FOV brighter pixels extracted from the black plane image histogram. Otherwise, t3 is determined using the percentage P3. This figure 3 shows that the work flow of the noise masks with black plane.

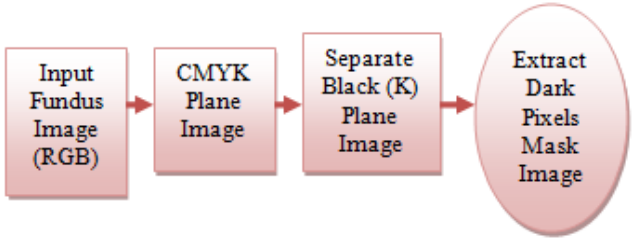


**Figure 3:** Work Flow of the NM with Black Plane

## 3. Focus Measure (FM)

It is a quantity which measures the degree of blurring of an image. Different focus measures have been proposed and used in auto focusing systems of digital cameras to determine the position of the best focused image [14-15]. In all focus measure are calculated by focused and blurred images. A good focus measure should satisfy following requirements:

1. Independence of image content.
2. Monotonicity with respect to blur.
3. Minimal computation complexity.
4. Robustness to noise.

### 3.1 Types of Focus Measure

1) Wavelet Focus Measure (WFM)
2) Moment Focus Measure (MFM)
3) Statistics Focus Measure (SFM)

#### 3.1.1 Wavelet FM

DWT (Discrete Wavelet Transform) has minimum no. of coefficients. By restricting scale and translation. Non-redundant & bilateral transform [16].

Forward DWT as in (1):

$$a_{jk} = \sum_{t} f(t)\psi^{*}_{jk}(t) \quad (1)$$

The discrete wavelet transform gives a multiresolution spatial frequency signal representation [17]. It measures functional intensity variations along the horizontal, vertical, and diagonal directions providing a simple hierarchical framework for interpreting the image information [18]. It is therefore natural to first analyze the image details at a coarse resolution and then gradually increase the resolution [19]. An image f(x,y) at an arbitrary starting scale j+1 is decomposed in its low frequency subband, Wφ(j,m,n) and high frequency subbands, WHψ(j,m,n), WVψ(j,m,n) and WDψ(j,m,n) where j represents the decomposition level and m and n are the columns and rows number, respectively in figure 4. Daubechies orthogonal wavelet basis D6 was used for computing FMwt. The wavelet-based focus measure used, FM (wt), is defined as the mean value of the sum of detail coefficients in the first decomposition level as in the form of the equation (2).

$$FM(wt)=(1/mn)\sum_{mn}[wH(1,m,n)+wV(1,m,n)+wD(1,m,n)] \quad (2)$$

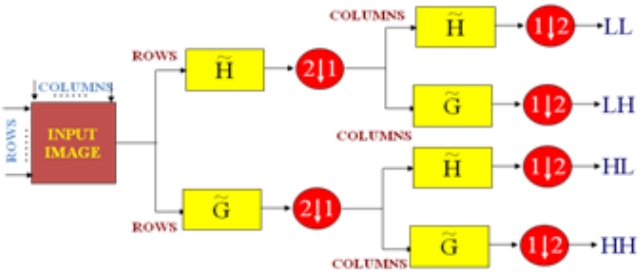


**Figure 4:** Wavelet Decomposition

#### 3.1.2 Moment FM

Image moments describe image content in a compact way and capture the significant features of an image. Moments, in the mathematical point of view, are projections of a function onto a polynomial basis. They have been used successfully in a variety of applications such as image analysis, pattern recognition, image segmentation, edge detection, image registration, among others. Two View of Moment Based FM:

1. Statistical view 2. Non-Statistical view

In Statistical View ,there are several types like mean, skewness, variance, correlation, kurtosis etc .In Non Statistical View, there are several families of orthogonal moments like chebyshev, legendre, krawtchouk, dual hann, fourier-mellin, Zernike moments etc. Orthogonal moments, due to its orthogonality property, simplify the reconstruction of the original function from the generated moments. In addition, orthogonal moments are characterized by being good signal and object descriptors, have low information redundancy and possess invariance properties, information compactness and transmission of spatial and phase information of an image. Here, we adopted a non statistical view of Zernike moment-based focus feature to "recognize" blurred images [20]. Zernike moment working in optics in the 1930 derived a set of polynomials that are orthogonal over a unit disk .This figure 5 shows that the first 15 Zernike polynomials, ordered vertically by radial degree and horizontally by azimuthally degree.

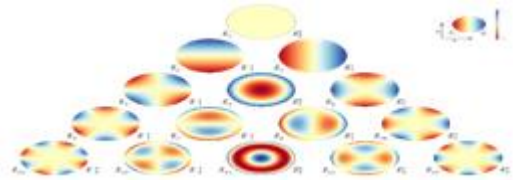

**Figure 5:** The First 15 Zernike Polynomials

There are specified in polar coordinates in terms of a radial component which is a polynomial of order. Their advantages: Simple rotation invariance, Higher accuracy for detailed shapes, Orthogonal, Less information redundancy. There are even and odd Zernike polynomials. The even ones and odd ones are defined as in (3) & (4).

$$Z_n^m(\rho,\varphi) = R_n^m(\rho)\cos m\varphi \quad (3)$$
$$Z_n^{-m}(\rho,\varphi) = R_n^m(\rho)\sin m\varphi \quad (4)$$

Where, m and n are nonnegative integers with $n \geq m$, φ is the azimuthally angle, here(φ=0),ρ is the radial distance. Zernike moments in terms of radial polynomial as in (5).

$$R_n^m(\rho) = \sum_{k=0}^{\frac{n-m}{2}} \frac{(-1)^k (n-k)!}{k!\left(\frac{n+m}{2}-k\right)!\left(\frac{n-m}{2}-k\right)!} \rho^{n-2k} \quad (5)$$

The zernike-based focus measure used, FM(zm), is defined as the ratio of higher order and lower order moments as in (6).

FM(zm)=higher order/lower order (6)

### 3.1.3 Statistics FM

The last focus measure applied to extract image content information uses a median filter and calculates the mean energy of the difference image. The median filter is normally used in preprocessing steps of fundus images analysis algorithms to reduce noise. This filter outperforms the mean filter since it preserves useful details of the image. The kernel size of the median filter was chosen as in corresponding to 1⁄30 the height of the fundus image. By subtracting the filtered image to the original green plane image, a difference image with enhanced edges is obtained, Idiff(x,y).This figure 6 shows that the work flow of the statistics based focus measure.

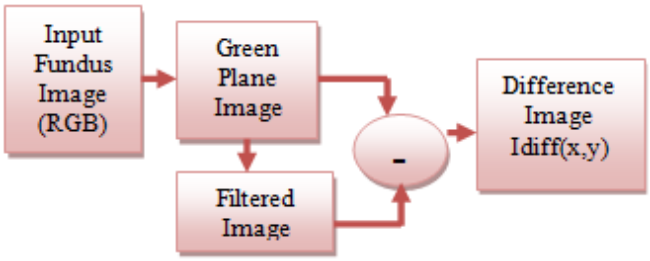


**Figure 6:** Work Flow of the Statistics Based Focus Measure

The statistics-based focus measure, FM(sta), is calculated using the following expression as in (7).

FM(sta)=$\sum_x \sum_y$[ Idiff (x,y)]^2 (7)

Finally, all focus measure values of focused and blurred images are plotted in Box Plot.

## 4. Box Plot or Whisker Plot

The box plot is defined by five data-summary values and also shows the outliers. The 25th percentile (Q1) is the value at which 25% of the data values are below this value. Thus, the middle 50 %( Q2) of the data values fall between the 25th percentile and the 75th percentile (Q3). The distance between the upper (75th percentile) and lower (25th percentile) lines of the box is called the inter-quartile range (IQR). IQR is a popular measure of spread. The IQR is $Q_3 - Q_1$ and measures the spread in the middle 50% of the data. This figure 7 shows that the box plot or whisker plot. To construct a box plot, we need only five statistics because we can predict the rules in this range.

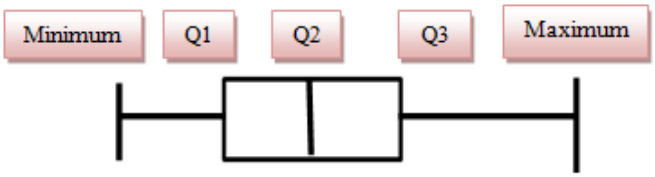


**Figure 7:** Box Plot or Whisker Plot

Location of percentile, Lp is calculated by using this formula as in (8).

Lp=(n+1)P/100 (8)

Where, n=Number of Observations

P=percentiles ($25^{th}$ or $50^{th}$ or $75^{th}$)

## 5. Classification

### 5.1 KNN Classifier

K-Nearest Neighbor (KNN) classifier is a simple supervised classification method. Suppose each sample in our data set has n attributes which we combine to form an n-dimensional vector: $x = (x_1, x_2 \ldots x_n)$. For the moment we will concern ourselves to the most popular measure of distance, Euclidean distance. The Euclidean distance between the points X and Y is calculated as in the form of equation (9).

Dist(X,Y)=$\sqrt{(\sum_i (X_i - Y_i)^2)}$ (9)

### 5.2 Fuzzy Classifier

A fuzzy classifier uses if-then rules which are easy to interpret by the user [21]. A fuzzy rule can be interpreted as a data behavior representation from which the fuzzy classifier was created, and is also known as Membership Functions (MF).

### 5.2.1 Fuzzy Inference Systems (FIS)

Fuzzy inference (reasoning) is the actual process of mapping from a given input to an output using fuzzy logic. The most important two types of fuzzy inference method are Mamdani and Sugeno fuzzy inference methods.Here we have chosen the Sugeno method [22] because we can predicted the limited number of rules. To generating fuzzy rules from an input-output data set, Sugeno fuzzy model was implemented into the neural fuzzy system. The most commonly used zero-order Sugeno fuzzy model applies fuzzy rules in the following

form of equation (10). This figure 8 shows that the sugeno model.

if x is A and y is B then z=k (10)

Where, A and B are fuzzy sets in the antecedent,

z =k is a function in the consequent part

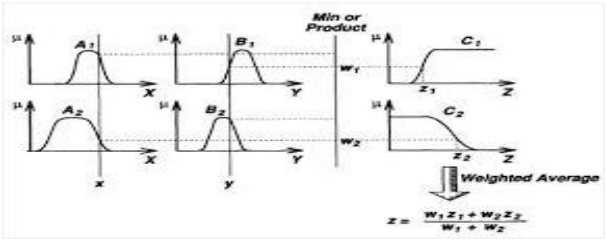


**Figure 8:** Sugeno Model

The system final output f(x) is calculated by the weighting average of all rule outputs as in (11).

$f(x) = \sum_{i=1}^{N}(wizi) / \sum_{i=2}^{N}(wi)$ (11)

**5.2.2 Adaptive Neuro-FuzzyInference Systems (ANFIS)**
A class of adaptive networks that are functionally equivalent to fuzzy inference systems. Here we adopted sugeno ANFIS. In this model every node i in this layer is an adaptive node with a node function O1,i = mAi (x), for I = 1,2, or O1,i = mBi-2 (y), for I = 3,4 Where x (or y) is the input to node i and Ai (or Bi) is a linguistic label O1,i is the membership grade of a fuzzy set. Every node i in this layer is a fixed node labeled P, whose output is the product of all the incoming signals:O2,i = Wi = min{mAi (x) , mBi (y)}, i = 1,2 Each node output represents the firing strength of a rule.O3,i = Wi = Wi /(W1+W2) , i =1,2 .The single node in this layer is a fixed node labeled S, which computes the overall output as the summation of all incoming signals: O 4,1 = ∑i wi fi.This figure 9 shows that the sugeno ANFIS model.

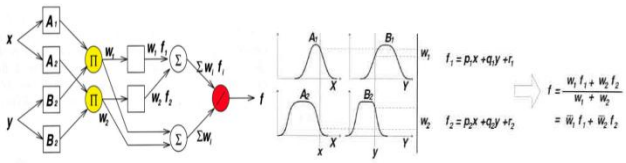

**Figure 9:** Sugeno ANFIS Model

## 6. Performance Evaluation

The classifier performance can be evaluated using receiver operating characteristic (ROC) analysis and the respective area under the curve (AUC). ROC curves plot the true positive fraction (or sensitivity) versus the false positive fraction (or one minus specificity). Sensitivity refers to the ability to classify an image as adequate related to focus, when it really is focused. Specificity refers to the capacity of classification of images out of focus as defocused. Accuracy was calculated by the fraction of images correctly assigned in the total number of classified images, at the operating point.
Sensitivity =TP/ (TP+FN) (12)
Specificity=TN/ (FP+TN) (13)
Accuracy = (TP+TN)/ (TP+TN+FP+FN)*100 (14)

Where, TP/TN→True Positive/True Negative
FP/FN→False Positive/False Negative

## 7. Results and Discussion

All processing blocks were implemented in MATLAB code, in version R2012. Database of fundus images were taken to MESSIDOR and to capture real time fundus images in Agarwal's Eye Hospital, Tirunelveli. Training set containing 382 images and the testing set containing 1072 retinal images for MESSIDOR. In real time fundus images, we have taken 100 images for training set and 175 images for testing set. The size of the MESSIDOR image is 2240 ×1488 and real time image is 1916 ×1664.

### 7.1 Preprocessing Result

This figure 10 shows that the preprocessing result. The left side of the RGB image is input image for MESSIDOR and Real time images and right of the image is extract the green component.

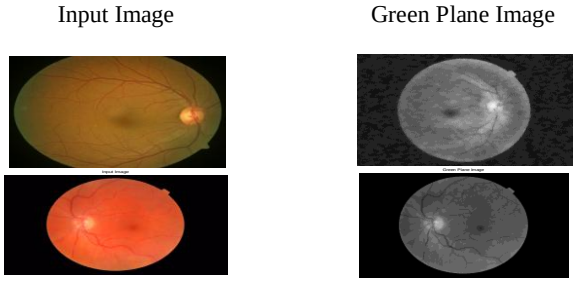


**Figure 10:** Preprocessing Result

### 7.2 Mask Result

This figure 11 shows that the mask result for clinically relevant and noise.


**Figure 11:** Mask Result

### 7.3 Focus Measure Result

The table 1 shows that the focus measure result for wavelet, zernike and statistical.

**Table 1:** Focus Measure Result

| Database | Images | WFM | Zernike MFM | SFM |
|---|---|---|---|---|
| MESSIDOR | Focused | 7.9E-05 | 0.0546 | -38 |
| | Blurred | 2.5E-05 | 0.076 | 20 |
| Real(Agarwal's Eye Hospital) | Focused | 3.7E-05 | 0.0744 | 17 |
| | Blurred | 1.9E-06 | 0.0088 | -15 |

### 7.4 Box Plot Result

This figure 12 shows that the box plot result for MESSIDOR and real images in WFM. Similarly, we have plotted the ZFM and SFM. In this plot we can predict and sorted the range of all three FM values.

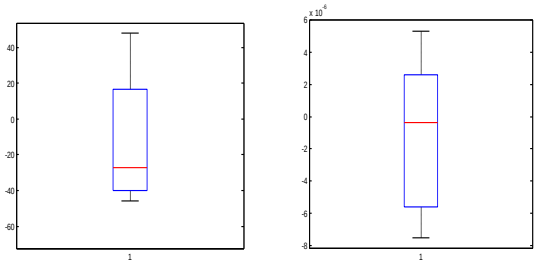

**Figure 12:** Box Plot Result

### 7.5 FIS Result

This figure 13 shows that the Sugeno FIS result.

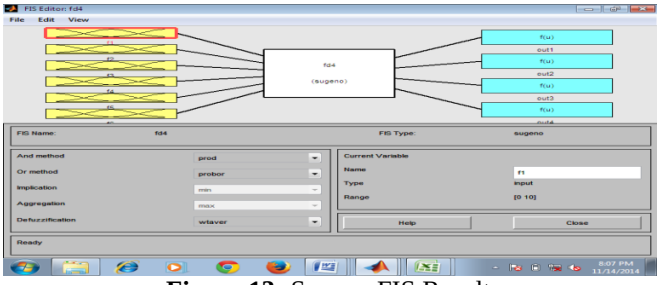

**Figure 13:** Sugeno FIS Result

### 7.6 ANFIS Result

This figure 14 shows that the Sugeno ANFIS result.

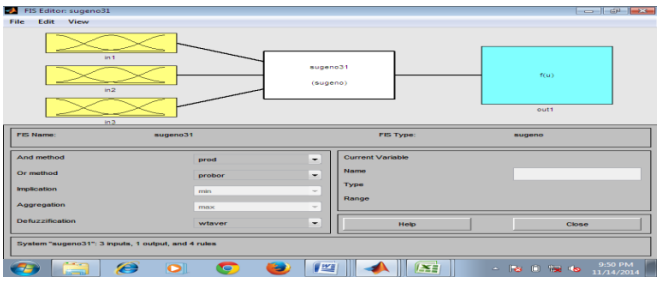

**Figure 14:** Sugeno ANFIS Result

### 7.7 ROC Plot Result

This figure 15 shows that the ROC plot result.

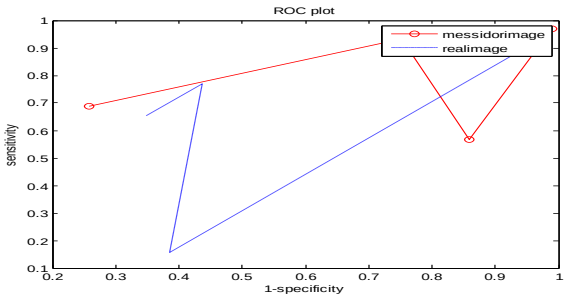


**Figure 15:** ROC Plot Result

### 7.7 Fuzzy Performance Result

This figure 16 shows that the fuzzy performance result.

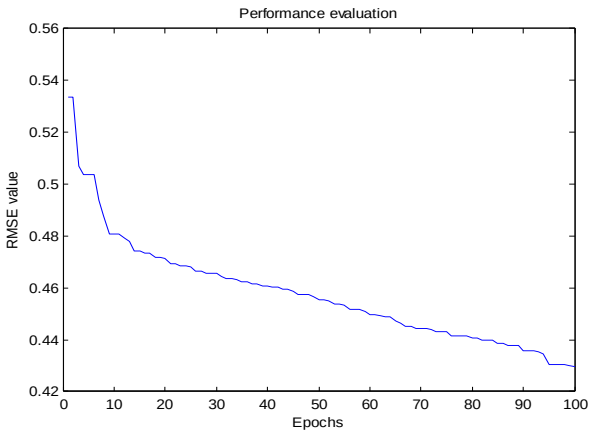


**Figure 16:** Fuzzy Performance Result

## 8. Conclusion

The present paper provides the preprocessing process can be done. Apply mask algorithm is to calculate the clinically relevant and noise mask, to verify the presence of uneven illumination and focus verification. Extract all focus measure value like wavelet, moment and statistics and it is marked as box plot or whisker plot .Then classifies the image quality is good or bad through classifier. Finally, KNN, Fuzzy classifiers (FIS & ANFIS) has been implemented and compared. The performance of these two classifiers has been analyzed. From that result, Fuzzy classifier gives better accuracy when compared with KNN classifier.

## Acknowledgement

I express my heartself gratitude to Dr. A. Heber M.Pharm. (Ph.D) Senior Clinical Research Manager in Dr Agarwal's Eye Hospital, Tirunelveli for providing the necessary facilities for conducting this research and his valuable suggestion its help me to greatly include this project work.

## References

[1] P.J. Saine, "Errors in fundus photography," J. Ophtalmic Photography, vol.7(2), pp.120–122, 1984.
[2] C.J. Heaven, J. Cansfield, K.M. Shaw, "The quality of photographs produced by the non-mydriatic fundus camera in a screening programme for diabetic retinopathy,": a 1 year prospective study Eye London England ;7(Pt 6):787-790, 1993.
[3] E. Trucco, "Validating retinal fundus image analysis algorithms: issues and a proposal," Investigative Ophthalmology Visual Science, vol.54(5), pp.3546–59, 2013.
[4] M Lalonde, L. Gagnon, M.C. Boucher, "Automatic visual quality assessment in optical fundus images," in Proceeding of Vision Interface 2001.
[5] T.J. Bennett & C.J. Barry, "Ophthalmic imaging today: an ophthalmic photographer's viewpoint—a review," clinical & experimental Ophthalmology, vol.37(1), pp.2–13, 2009.

[6] S. Lee, & Y. Wang, "Automatic retinal image quality assessment and enhancement", Proceeding SPIE, vol.3661, pp.1581–1590, 1999.
[7] D.B. Usher, M. Himaga, M.J. Dumskyj, "Automated assessment of digital fundus image quality using detected vessel area," Proceedings of Medical Image Understanding and Analysis 2003.
[8] A.D. Fleming, S. Philip, K.A. Goatman, J.A. Olson, P.F. Sharp, "Automated assessment of diabetic retinal image quality based on clarity and field definition," Investigative Ophthalmology & Visual Science ;47:pp.1120-1125, 2006.
[9] T.D. Kite, "Design quality assessment of forward and inverse error difusion halftoning algorithm," Ph. D. thesis, University of Texas at Austin 1998.
[10] H. Yu, S. Barriga, C. Agurto, G. Zamora, W. Bauman, and P. Soliz, "Fast Vessel Segmentation in Retinal Images Using Multiscale Enhancement and Second-order Local Entropy," accepted by SPIE medical imaging, Feb, San Diego, USA 2012.
[11] H. Bartling, P. Wanger, L Martin, "Automated quality evaluation of digital fundus photographs," Acta Ophthalmologica, vol. 87(6), pp. 643–647, 2009.
[12] J.M. Pires Dias, C.M. Oliveira, L.A. da Silva Cruz, "Retinal image quality assessment using generic image quality indicators," Information Fusion, vol.19, pp.73–90, 2014.
[13] N. Otsu, "A Threshold Selection Method from Gray-Level Histograms," IEEE Trans. Syst. Man and Cybern., pp. 62-66, 1979.
[14] D. Veiga, "Focus evaluation approach for retinal images," in VISAPP—VISIGRAPP, SCITEPRESS Digital Library 2014.
[15] X. Wang, & Y. Wang, "A new focus measure for fusion of multi-focus noisy images," in International Conference on Computer, Mechatronics, Control and Electronic Engineering, vol. 6, pp.3–6, IEEE, Changchun 2010.
[16] R.C. Gonzalez, & R.E. Woods, Digital Image Processing 3rd ed., Pearson Prentice Hall 2008.
[17] S. Jayaraman, S. .Esakkirajan, T. Veerakumar, Digital Image Processing, Tata McGraw Hill Education Private Limited 2013.
[18] S. Mallat, "A theory for multi resolution signal decomposition: the wavelet representation," Pattern Analysis Machine Intelligence IEEE Transaction, vol.11(7), pp.674–693, 1989.
[19] G. Yang, & B. Nelson, "Wavelet-based autofocusing and unsupervised segmentation of microscopic images," in International Conference on Intelligent Robotics and Systems Proceedings of the IEEE/RSJ, vol.3, pp.2143–2148 2003.
[20] A. Khotanzad, & Y.H. Hong,"Rotation invariant pattern recognition using Zernike moments," ICPR,Cambridge, UK, pp. 326-328, 1988.
[21] A. Hoover, & M. Goldbaum, "Locating the Optic Nerve in a Retinal Image using the Fuzzy Convergence of the Blood Vessels," IEEE Trans. Med. Imag. 22, pp.951-958 2003.
[22] D. Nauck, & R. Kruse, "Obtaining interpretable fuzzy classification rules from medical data," Artificial Intelligence Medicine, vol.16(2), pp.149–169, 1999.
[23] Mathworks, Fuzzy Logic Toolbox: Adaptive Neuro fuzzy Modelling (R2012b) 2012